A FORWARD MODELING OF INFRARED REFLECTANCE SPECTRA OF ASTEROIDS: THE IMPLICATIONS FOR RYUGU'S PALENT BODY. H. Kurokawa[1*], T. Shibuya[2], Y. Sekine[1], and B. L. Ehlmann[3], [1]ELSI, Tokyo Tech, [2]JAMSTEC, [3]Caltech/JPL, *hiro.kurokawa@elsi.jp.

Introduction: The mineral assemblages on asteroids are useful to constrain the aqueous environments ―the temperature (*T*), pressure (*P*), water to rock ratio (W/R), and bulk chemical composition―existed in them or in their parent bodies. The aqueous conditions reflect their formation and evolution processes: when, where, and how they have formed and evolved. The understandings of these small bodies would ultimately unveil the dynamic history of the early solar system as well as the origins of volatile elements on Earth.

Near- to mid-infrared (IR) reflectance spectroscopy of asteroids contains the information of the surficial minerals in their characteristic absorption features, spectral slopes, and overall brightness or darkness. Recent remote-sensing of asteroids by Hayabusa2, OSIRIS-Rex, and Dawn spacecrafts as well as telescopic observations by AKARI infrared space telescope provided detailed IR reflectance spectra of many types of asteroids [1-4]. These observations would allow us to discuss the diversity of asteroids in their principle parameter space of paleo-aqueous environments: *T*, *P*, W/R, and the bulk chemical compositions.

This study aims to connect the observed IR spectra of asteroids to the original bulk compositions and *T*-*P* conditions of them or their parent bodies. We performed a series of chemical equilibrium calculations to obtain the mineral compositions. We computed the model IR reflectance spectra from the obtained mineral compositions. In this presentation, we especially discuss the implications for the parent body of Ryugu.

Model: The chemical equilibrium calculations assumed the rocky bulk compositions of CV chondrites. We treated W/R as a parameter (0.2-10). We fixed the relative abundance of volatiles to water. Model 1 assumed a pure water and rock mixture. Models 2 and 3 assumed CO_2: 1 and 3%, NH_3: 0.5%, and H_2S: 0.5% relative to water. The temperature is a parameter (T = 0 °C cases are shown in this abstract) and *P* equals the saturation vapor pressure of water. We used EQ3/6 computation software. In our model, pyrene represents organic phases, which would eventually form high-molecular-weight insoluble-organic-matter (IOM) typically found in meteorites.

The model IR reflectance spectra were calculated by adopting the radiative transfer theory for granular surfaces [5]. The reflectance of a model mineral assemblage was computed from the weighted average of the single scattering albedos (SSAs) of endmembers. The endmember SSAs were calculated from their reflectance spectra taken from RELAB database and [6-7]. We used the reflectance for the sample size range of 0–45 μm when available. Otherwise the reflectance for this size ranges were computed by using optical constants estimated from the informed reflectance data for other sizes. We assumed that grains are spherical, isotropic scatters. We employed the incident angle i = 30° and the emergence angle e = 0°, respectively.

Results: The chemical equilibrium calculations showed that abundant hydrous minerals are formed when T = 0–300 °C (Figure 1a), whereas anhydrous minerals become dominant for higher T (not shown). As W/R becomes lower, carbonate is converted into organics (CO_2-reduction) in Models 2 and 3. Eventually, magnetite dominates over organics. Ammonia-bearing saponite appears at W/R > ~1, T < ~100 °C, and high CO_2 conditions. In contrast, higher T conditions favor Fe-smectite because the acidic pH increases the metal concentration in fluid. Further results of the chemical equilibrium calculations will be presented in [8].

The model reflectance spectra vary according to the equilibrium mineral compositions (Figure 1b). Reducing W/R in Models 2 and 3 led to the darkening in overall reflectance as the dominant minerals change from bright carbonate to serpentine, gibbsite, and dark phases―pyrite, troilite, magnetite, and organics. The change in the dominant phase is visible in the characteristic absorption features: carbonate at 3.5 μm and 4.0 μm and serpentine at 2.7-2.8 μm. We note that, though carbonate has a broad absorption from 2.7 to 3.2 μm, the absorption feature of serpentine is sharp and distinguishable. Ammonia-bearing saponite more than a few wt.% shows its characteristic absorption feature at 3.1 μm in the reflectance of mixture.

Our model reproduced the reflectance patterns of chondrites qualitatively: CI chondrite (Ivuna) like sharp 2.7 μm absorption and 3,5 and 4.0 μm features when W/R~2-5 in Models 2 and 3, and CM chondrite (e.g., Cold Bokkeveld) like 2.7 μm absorption when W/R < 1 (Figure 1b). These results are consistent with isotopically-estimated W/R of carbonaceous chondrites (CCs) [9].

Discussion: The Near Infrared Spectrometer (NIRS3) onboard Haybusa2 observed asteroid Ryugu at wavelengths of 1.8 to 3.2 μm. The IR reflectance is very low (~0.02) and mostly uniform over the surface. The spectra contain a confirmed sharp absorption at 2.72 μm and unconfirmed possible absorption at 3.05 μm. Both of them have the relative absorption depth ~0.1. In addition, the Optical Navigation Camera (ONC) found localized bright materials.

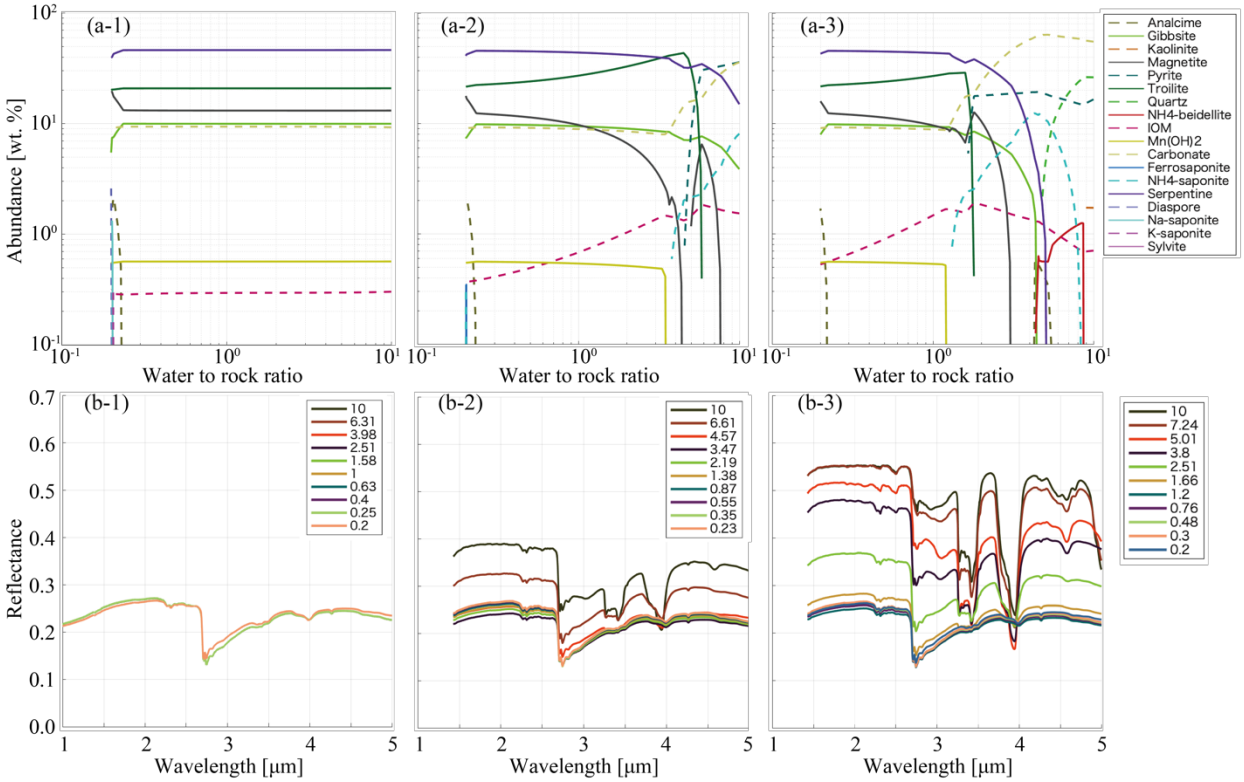

Figure 1. a: The mineral abundances as a function of W/R obtained from the chemical equilibrium calculations. Panels a-1, a-2, and a-3 show the results for CO_2 to water ratio = 0, 1, and 3%, respectively (Models 1-3). Models 2 and 3 contain NH_3 and H_2S in the starting materials (see text). b: The model IR reflectance spectra of mineral assemblages. Lines correspond to the spectra for different W/R shown in the legends. Panels b-1, b-2, and b-3 show the results for Models 1-3, respectively.

Combining NIRS3's data to our results constrain the aqueous environment in Ryugu's parent body. Though NIRS3 does not cover the range where carbonate absorption exists (3.5 μm and 4.0 μm), the sharpness of 2.7 μm absorption indicates hydrous minerals such as serpentine (Figure 1b). The 3.05 μm absorption, if exists, suggests the presence of NH_4-bearing phases such as NH_4-saponite or other NH_4 clay minerals. The overall low reflectance requires darkening materials (sulfide, IOM, and magnetite). The IR spectra of localized bright materials on Ryugu have not been measured yet. A possible bright mineral assemblage is a carbonate-rich composition.

The dominance of dark phases and serpentine rather than carbonate suggests W/R < ~1 (Figure 1a). The weakness of 2.7 μm may imply a low abundance of hydrous phases, which requires $T < 0$ °C or $T > 300$ °C, or late dehydration. The abundant dark phases may suggest the late dehydration (due to solar irradiation and/or impacts) scenario following the reaction at $T = 0$–300 °C. Ammonia-bearing phases, if confirmed, further constrain the condition to W/R~1 and $T <$ ~100 °C. The bright region on Ryugu may sample a region in the parent body (W/R > ~1) different from that of the average surface.

Though our model showed a trend to the lower reflectance (~0.2) as dark materials become abundant, Ryugu has a much lower reflectance (~0.02). Ryugu is as dark as the darkest CCs, whose darkening mechanism has not been fully elucidated. Carbon has been widely considered to be the major darkening agent [10], though other dark phases also contribute the low reflectance [11]. The darkest CCs contain ~4 wt.% carbon chiefly as IOM [11,12]. If we employ this empirical relation, the starting materials are needed to be rich in carbon (Figure 1a). We note that factors other than mineralogy (e.g., grain sizes, H/C ratio of IOM) also control the reflectance.

References: [1] Iwata, T. et al. (2017) *SSR*, 208, 317-337. [2] Reuter, D. C. et al. (2018) *SSR*, 214, 54. [3] De Sanctis et al. (2015) *Nature*, 528, 241-244. [4] Usui, F. et al. (2018) PASJ, https://doi.org/10.1093/pasj/psy125. [5] Hapke, B. (2012) *Cambridge University Press*. [6] Ehlmann, B. L. et al. (2018) *MPS*, https://doi.org/10.1111/maps.13103. [7] Kaplan, H. H. et al. (2018) *GRL*, 45, 5274–5282. [8] Shibuya, T. et al. (2019) *50th LPSC*. [9] Marrocchi, Y. et al. (2018) *EPSL*, 482, 23-32. [10] Cloutis, E. A. et al. (2012) *Icarus*, 221, 328-358. [11] Garrene, A. et al. (2016) *Icarus*, 264, 172-183. [12] Alexander, C. M. O'D. et al. (2012) *Science*, 337, 721-723.